Definition of an intramolecular Eu-to-Eu energy transfer within a discrete [Eu2L] complex in solution[i]

Aline Nonat[a], Martín Regueiro-Figueroa[b], David Esteban-Gómez[b], Andrés de Blas[b], Teresa Rodríguez-Blas[b], Carlos Platas-Iglesias[b], Loïc J. Charbonnière[a*]

[a] Laboratoire d'Ingénierie Moléculaire Appliquée à l'Analyse, IPHC, UMR 7178 CNRS/UdS, ECPM Bâtiment R1N0, 25 rue Becquerel, 67087 Strasbourg Cedex (France)

[b] Departamento de Química Fundamental, Universidade da Coruña, Campus da Zapateira, Rúa da Fraga 10, 15008 A Coruña (Spain)

Chemistry – A European Journal, volume 18, issue 26, pages 8163–8173, 25 June 2012
Received 09 January 2012, version of record online 21 May 2012, issue online 18 June 2012

Abstract

Ligand L, based on two do3a moieties linked by the methylene groups of 6,6′-dimethyl-2,2′-bipyridine, was synthesized and characterized. The addition of Ln salts to an aqueous solution of L (0.01 M Tris-HCl, pH 7.4) led to the successive formation of [LnL] and [Ln_2L] complexes, as evidenced by UV/Vis and fluorescence titration experiments. Homodinuclear [Ln_2L] complexes (Ln=Eu, Gd, Tb, Yb, and Lu) were prepared and characterized. The ^{1}H and ^{13}C NMR spectra of the Lu and Yb complexes in D_2O solution (pD=7.0) showed C_1 symmetry of these species in solution, pointing to two different chemical environments for the two lanthanide cations. The analysis of the chemical shifts of the Yb complex indicated that the two coordination sites present square antiprismatic (SAP) coordination environments around the metal ions. The spectroscopic properties of the [Tb_2L] complex upon ligand excitation revealed conventional behavior with τ_{H2O}=2.05(1) ms and ϕ_{H2O}=51 %, except for the calculation of the hydration number obtained from the luminescent lifetimes in H_2O and D_2O, which pointed to a non-integer value of 0.6 water molecules per Tb^{III} ion. In contrast, the Eu complex revealed surprising features such as: 1) the presence of two and up to five components in the $^{5}D_0 \rightarrow {}^{7}F_0$ and $^{5}D_0 \rightarrow {}^{7}F_1$ emission bands, respectively; 2) marked differences between the normalized spectra obtained in H_2O and D_2O solutions; and 3) unconventional temporal evolution of the luminescence intensity at certain wavelengths, the intensity profile first displaying a rising step before the occurrence of the expected decay. Additional spectroscopic experiments performed on [$Gd_{2-x}Eu_xL$] complexes (x=0.1 and 1.9) confirmed the presence of two distinct Eu sites with hydration numbers of 0 (site I) and 2 (site II), and showed that the unconventional temporal evolution of the emission intensity is the result of an unprecedented intramolecular Eu-to-Eu energy-transfer process. A mathematical model was developed to interpret the experimental data, leading to

* l.charbonn@unistra.fr

energy-transfer rates of 0.98 ms^{-1} for the transfer from the site with q=0 to that with q=2 and vice versa. Hartree–Fock (HF) and density functional theory (DFT) calculations performed at the B3LYP level were used to investigate the conformation of the complex in solution, and to estimate the intermetallic distance, which provided Förster radii (R_0) values of 8.1 Å for the energy transfer from site I to site II, and 6.8 Å for the reverse energy transfer. These results represent the first evidence of an intramolecular energy-transfer equilibrium between two identical lanthanide cations within a discrete molecular complex in solution.

Keywords: energy transfer; europium; lanthanides; luminescence; macrocyclic ligands

Introduction

Energy-transfer (ET) processes are of fundamental importance both for the understanding of natural phenomena such as the photon funneling of the photosynthetic systems of some bacteria,[1,2] and for the development of synthetic scaffolds such as photoactive polymer-based sensors,[3,4] solar concentrators,[5] or fluorescence-based immunogenic assays.[6,7]

ET processes are generally resonant processes between isoenergetic levels of a donor and an acceptor, sometimes assisted by interaction with phonons,[8] and are usually accompanied by energy losses that result in a bathochromic shift of the energy output. Such processes have mainly been studied within the framework of dipole–dipole (Förster)[9] or exchange (Dexter)[10] formalisms, to account for ET processes within organic or inorganic molecules.[11–13] In a few cases, particularly those where the high photon flux generates a large population of excited states, ET processes can occur directly between excited states, leading to an output signal at a higher energy than the input, i.e., up-converting processes.[14,15]

Cases in which the ET process occurs between two isoenergetic levels are rather rare, not only because they require photoactive entities deprived of a Stokes' shift (no energy difference between the absorption and emission of photons), but also because it becomes difficult to discriminate the information arising from each entity when their spectral characteristics (such as absorption and emission spectra) are similar. Lanthanide complexes appear to be good candidates for possible isoenergetic ET. Their electronic transitions involve $4f^n$ orbitals (n=1–13), which are shielded from interaction with the environment by the filled $5p^6 6s^2$ sub-shells.[16] Their corresponding excited states are only weakly affected by the ligand field or by interaction with solvent molecules, resulting in narrow emission bands that are characteristic of each lanthanide cation. In contrast, the luminescence lifetimes of lanthanide complexes are very sensitive to quenching processes arising from vibrational deactivation through NH, OH, and CH oscillators.[17] Hence, despite the similar spectral signatures of two isoelemental Ln complexes, they may be distinguished on the basis of their luminescence lifetimes. ET processes between identical Ln^{III} cations in different environments have been reported for solid-state compounds,[18] but no such example has yet been found for discrete molecular entities in solution.

We report here that the complexation of Eu^{III} cations by a symmetrical ligand based on two do3a moieties linked by a 6,6′-dimethyl-2,2′-bipyridine unit resulted in a [Eu_2L] complex with two different coordination sites. Within this complex, an unprecedented example of Eu-to-Eu back-and-forth energy transfer was observed in aqueous solution. The process was established unambiguously by a combination of photophysical experiments, and a mathematical treatment was developed to account for the ET phenomenon.

Results and discussion

Synthesis and characterization of the ligand and Ln^{III} complexes

The synthetic procedure used for the preparation of L and its Ln^{III} complexes is outlined in Scheme 1. The synthesis of the ligand was achieved in three steps from 6,6′-dimethyl-2,2′-bipyridine, which was converted to the bromomethyl derivative **1** by free-radical bromination with dibenzoylperoxide and *N*-bromosuccinimide (NBS). *N*-alkylation of do3a(*t*BuO)$_3$[19] with **1** in acetonitrile under reflux conditions in the presence of Na_2CO_3 gave compound **2** in good yield (85 %). Full deprotection of the *tert*-butyl esters of **2** was achieved cleanly with a CF_3COOH:H_2O (1:1) mixture to give the desired ligand as the hexatrifluoroacetate salt (75 % yield). Reaction of $H_6L{\cdot}6\,CF_3COOH$ with lanthanide triflates in the presence of an excess of triethylamine resulted in the formation of compounds of the formula $[Ln_2L]{\cdot}4\,H_2O$ (Ln=Eu, Gd, Tb, Yb, or Lu), which were isolated in 77–85 % yields. The high-resolution mass spectra (ESI^+) showed peaks due to the $[Ln_2L+2\,H]^{2+}$ and $[Ln_2L+H]^+$ entities, thereby confirming the formation of the desired complexes (Figures S3–S7, Supporting Information).

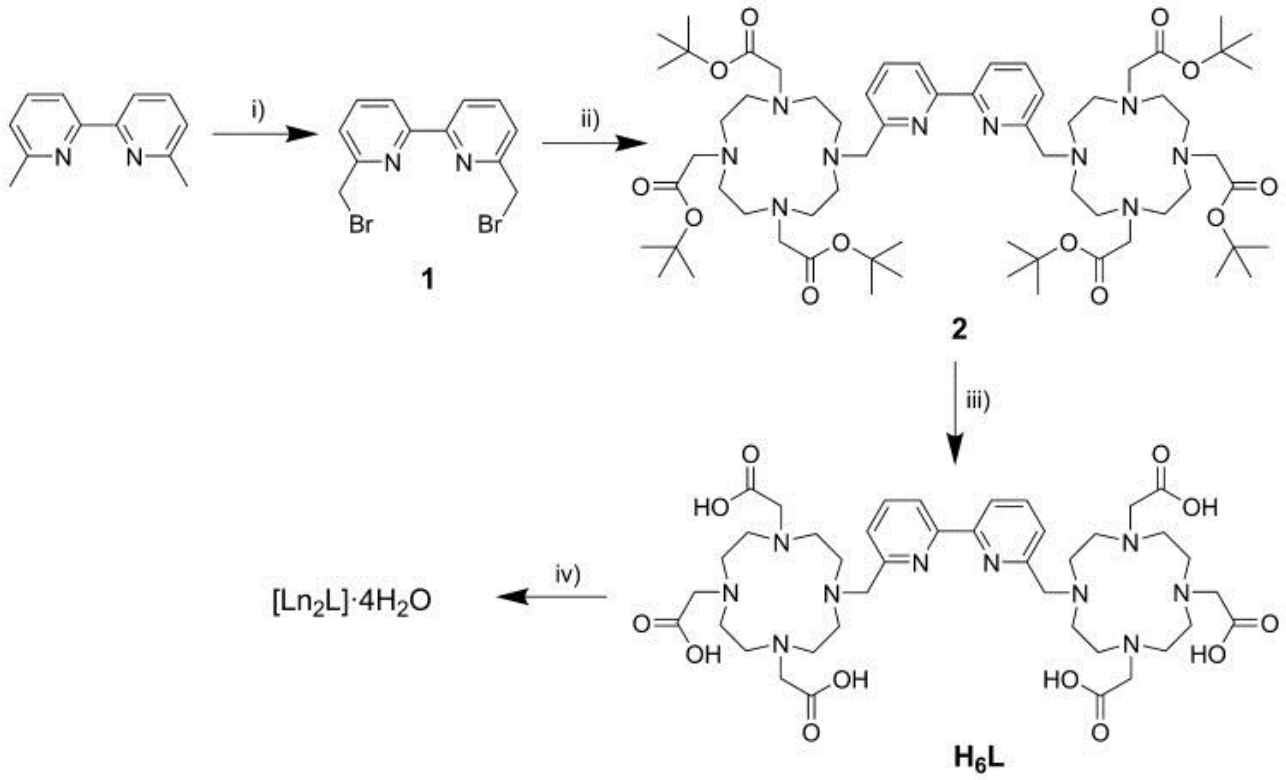

Scheme 1. i) NBS, dibenzoyl peroxide, CCl_4; ii) do3a(*t*BuO)$_3$, Na_2CO_3, CH_3CN; iii) CF_3COOH:H_2O (1:1); iv) $Ln(CF_3SO_3)_3$, Et_3N, 2-propanol.

Structures of the complexes in solution

The ^1H spectrum of the diamagnetic $[Lu_2L]$ complex recorded in D_2O solution (500 MHz, 298 K, pD 7.0) shows six signals in the range 8.16–7.59 ppm, together with relatively broad signals in the region 5.32–2.27 ppm, which are typical of Ln^{III} complexes with *N*-alkylated do3a derivatives.[20] The corresponding ^{13}C NMR spectrum, however, is well resolved, and consists of 46 signals: 6 signals in the range 183.3–180.5 ppm due to the carbonyl groups, 10 signals between 161.3 and 124.5 ppm arising from the carbon nuclei of the bipyridyl unit (Figure 1), and 24 signals in the region 68.2–46.8 ppm due to the $–CH_2–$ groups of the

ligand. This pattern points to a C_1 symmetry of the complex in solution, and suggests that the two Lu^{III} ions present different coordination environments. The ^{1}H NMR spectrum of the paramagnetic [Yb_2L] complex (300 MHz, 298 K, pD 7.0) is also in agreement with C_1 symmetry in solution. It shows 54 paramagnetically shifted signals ranging between 160.1 and −122.5 ppm (Figure 1). The eight non-equivalent resonances in the range 110–161 ppm may be assigned to pseudo-axial protons on the cyclen rings. The chemical shifts of these signals are characteristic of square antiprismatic (SAP) coordination geometries around the two metal ions, as determined by comparison with related compounds.[21]

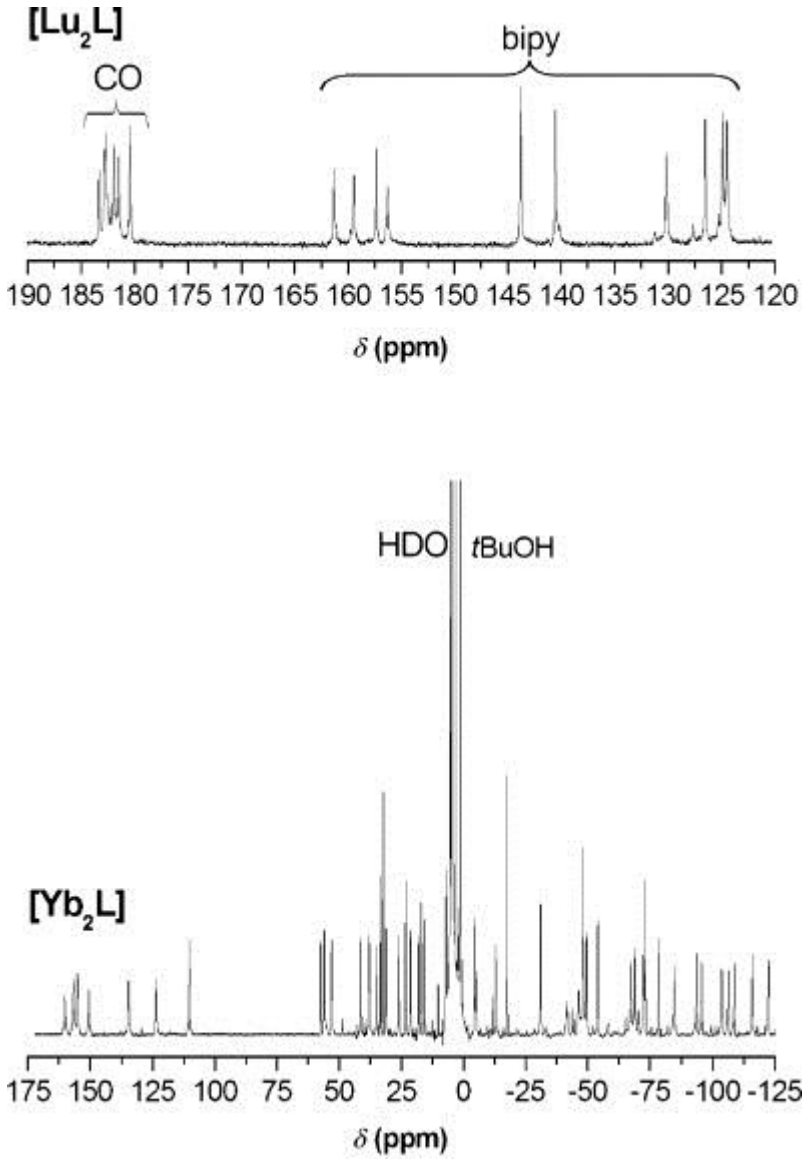

Figure 1. Top: Partial ^{13}C NMR spectrum of [Lu_2L] recorded in D_2O solution (125.8 MHz, 298 K, pD 7.0). Bottom: ^{1}H NMR spectrum of [Yb_2L] recorded in D_2O solution (300 MHz, 298 K, pD 7.0).

Spectrophotometric titration of the ligand by Eu^{III}

To gain insights into the complexation behavior of ligand L toward the lanthanide cations, we performed spectrophotometric titrations in which we monitored the changes in the absorption and emission spectra of L upon addition of $EuCl_3$. To avoid any trouble inherent to the slow complexation kinetics of the macrocyclic ligand, we added aliquots of a $EuCl_3$ stock solution to solutions containing a constant

concentration of ligand L (final concentration 5×10^{-5} M in 0.01 M Tris-HCl buffer at pH 7.0), and the mixtures were heated for 5 h at 60 °C and 64 h at 45 °C so that they reached thermodynamic equilibrium. The changes observed in the UV/Vis absorption spectra are presented in Figure 2.

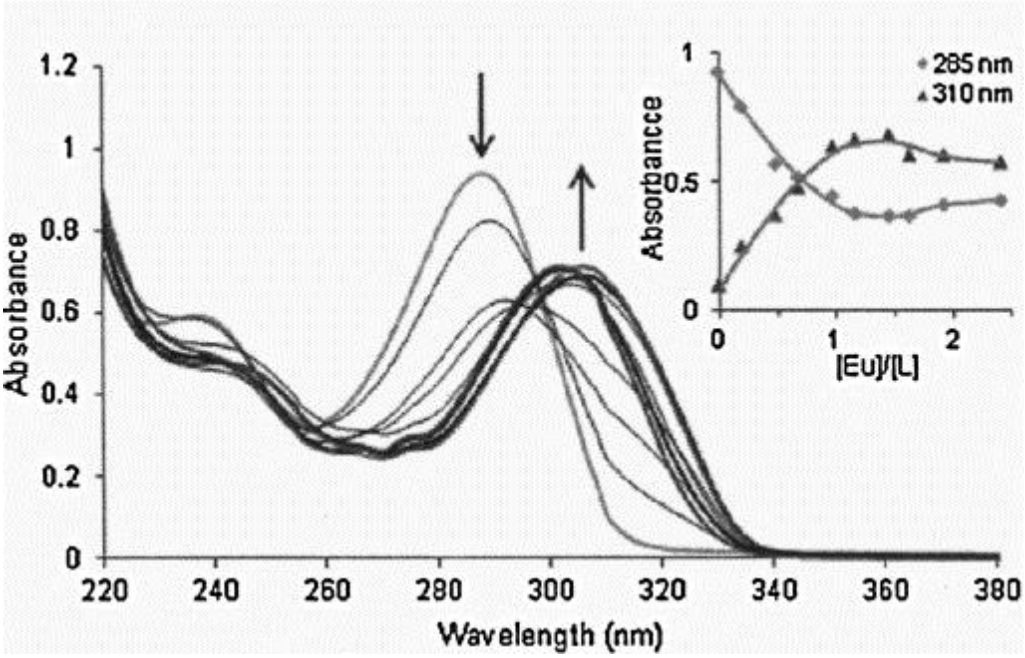

Figure 2. Evolution of the UV/Vis absorption spectra of an aqueous solution of L (c=4.99×10^{-5} M, TRIS-HCl 0.01 M at pH 7.0) upon addition of increasing amounts of $EuCl_3\cdot6\,H_2O$ (uncorrected for dilution). Inset: Evolution of the absorbances at 285 and 310 nm as a function of the [Eu^{III}]/[L] ratio and the corresponding fit (see text).

Upon addition of Eu^{III}, the strong absorption band centered at 287 nm was bathochromically shifted, with its maximum observed at 306 nm upon addition of 1.1 equivalents of $EuCl_3\cdot6\,H_2O$. These changes are indicative of the formation of a mononuclear [EuL] species, which is accompanied by the isomerization of the bipyridine unit from the *trans* conformation for L to a *cis* conformation in [EuL].[22] Upon addition of the second equivalent of Eu^{III}, a small hypsochromic shift from 306 nm to 300 nm was observed, pointing to the formation of a [Eu_2L] complex with a distorted *cis* conformation of the bipyridyl unit. These changes could be studied by an evolving factor analysis with the Specfit software,[23] and were satisfactorily fitted to a binding model in which the species are formed according to Equations (a) and (b) (charges are omitted for the sake of clarity):

$$\mathrm{Eu} + \mathrm{L} \leftrightarrow [\mathrm{EuL}] \quad K_{11} = [\mathrm{EuL}]/[\mathrm{Eu}][\mathrm{L}] \tag{a}$$

$$\mathrm{Eu} + [\mathrm{EuL}] \leftrightarrow [\mathrm{Eu_2L}] \quad K_{21} = [\mathrm{Eu_2L}]/[\mathrm{Eu}][\mathrm{EuL}] \tag{b}$$

Figure 3 displays the calculated spectra of the species formed during the titration and the evolution of the concentrations of the species observed.

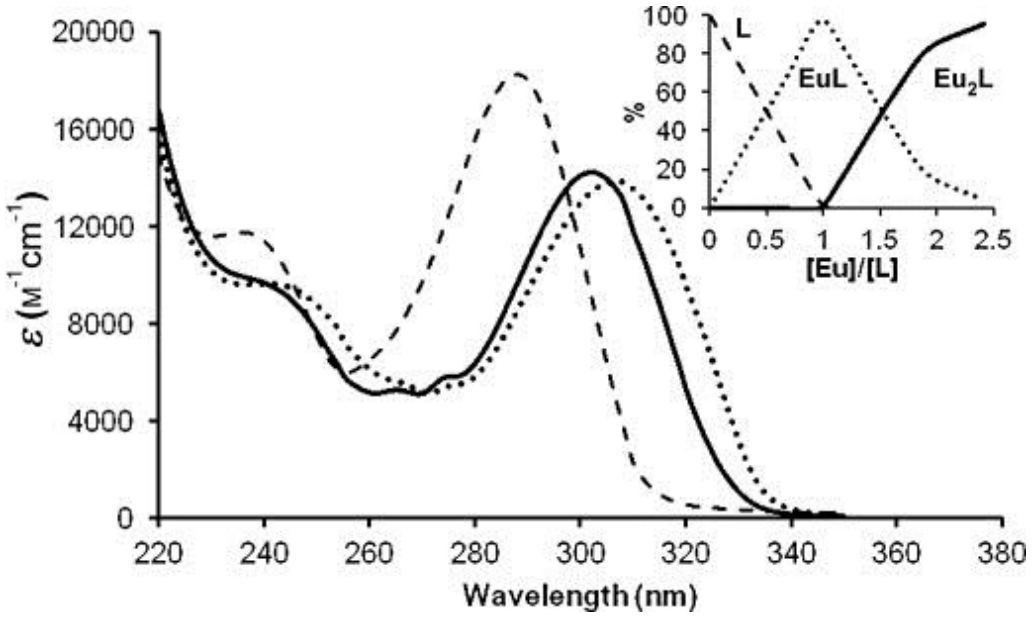

Figure 3. Calculated UV/Vis absorption spectra of the species formed during the titration of L by $EuCl_3 \cdot 6\,H_2O$ in 0.01 M Tris-HCl at pH 7.0. Inset: evolution of the concentration of the species during the titration.

The same titration experiment was followed by fluorescence spectroscopy, performed by monitoring the Eu^{III} emission in the 550–750 nm region upon excitation at 300 nm. From 0 to 2 equivalents, the Eu^{III} emission intensity gradually increased. The data were similarly fitted with the regression analysis software Specfit, and the results of the fitting were in good agreement with the data obtained by absorption spectroscopy. Both titrations were in agreement with particularly high binding constants, as expected for such a cyclen-based ligand. As a comparison, a stability constant of $\log K_{11}=23.5$ was previously measured for $[Eu(DOTA)]^-$.[24] Although the formation constant of the 1:1 complex is too high to be determined by using direct titration experiments ($\log K_{11}>6$), the apparent stepwise formation constant of $\log K_{21}=6.1(6)$ could be determined for the second complexation step.

Spectroscopic properties of the $[Tb_2L]$ complex

The photophysical properties of the binuclear $[Tb_2L]$ complex were studied in solution and in the solid state. The UV/Vis absorption spectrum of $[Tb_2L]$ in a 0.01 M Tris-buffered aqueous solution (pH 7.4) displays a broad absorption band with a maximum at 301 nm (ε=10 920 $M^{-1}\,cm^{-1}$), which is typical of $\pi\rightarrow\pi^*$ transitions centered on the bipyridine units, and a shoulder at approximately 240 nm (ε=6 880 $M^{-1}\,cm^{-1}$ at 238 nm, Figure 4). As stated before, the intense $\pi\rightarrow\pi^*$ transition centered at 301 nm is indicative of a distorted *cis* conformation of the two pyridine rings.[22]

Upon excitation into the absorption band in the UV/Vis domain, the complex displays an emission pattern characteristic of the $^5D_4\rightarrow{}^7F_J$ (J=6–3) transitions of Tb^{III} ions (Figure 4).[25] No residual fluorescence of the ligand could be observed. The excitation and UV absorption spectra are very similar, which strongly supports efficient ligand-to-metal energy transfer.

The luminescence decay profiles of $[Tb_2L]$ were recorded in phosphorescence mode, and could be fitted conveniently with monoexponential decays. From the measured lifetimes in H_2O (τ_{H2O}=2.05 ms) and D_2O (τ_{D2O}=3.18 ms), a hydration number of q=0.6±0.2 was determined.[17a] This value strongly suggests a mixture of species with different hydration states in solution. Sensitized emission quantum yields of ϕ_{H2O}=51 % and ϕ_{D2O}=57 % were determined in 0.01 M Tris-HCl buffered aqueous solutions (pH 7.4) and in D_2O, respectively, using rhodamine 6G (ϕ_{H2O}=76 %) in water as a reference.[26] The emission spectrum

of [Tb_2L] was also measured in the solid state, and the corresponding quantum yield determined using an absolute method[27] was ϕ_{solid}=24 %.

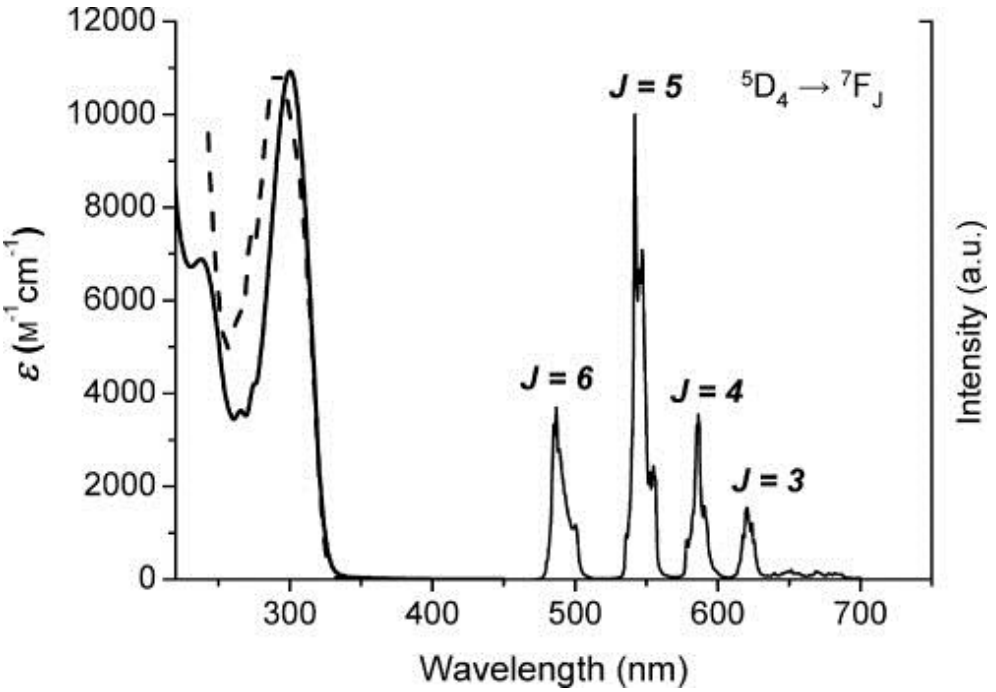

Figure 4. UV/Vis absorption (solid line, left part), excitation (dotted lines, λ_{em}=545 nm) and high-resolution emission spectrum (λ_{ex}=300 nm, right part) recorded for [Tb_2L] in aqueous solutions (0.01 M Tris-HCl buffer, pH 7.4, c=1.5×10^{-5} M).

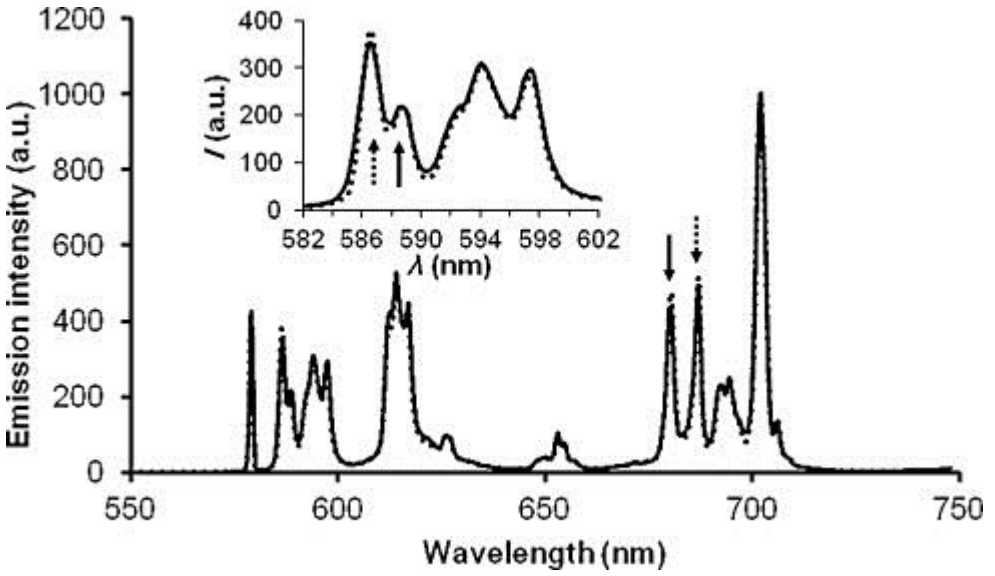

Figure 5. Normalized experimental (—) and calculated (···) emission spectra of [EuL] upon excitation at 300 nm in 0.01 M Tris-HCl, pH 7.0. [Arrows and dotted arrows refer to TSAP and SAP spectral signatures, respectively (see text and ref. 27)].

Spectroscopic properties of the [EuL] and [Eu_2L] complexes

The spectroscopic characterization of [EuL] was performed for an equilibrated solution containing ligand L and 0.1 equivalents of $EuCl_3 \cdot 6\,H_2O$. Under these conditions, the mononuclear species represents more than 99 % of the complexed Eu^{III} in solution according to the spectrophotometric titration experiments (see above). The Eu^{III} emission spectrum was measured upon excitation at 300 nm, and is in good agreement with the calculated spectrum obtained from the titration data (Figure 5). The emission spectrum displays the characteristic bands associated with the $^5D_0 \rightarrow {}^7F_J$ (J=0–4) transitions. At least five components are observed for the $^5D_0 \rightarrow {}^7F_1$ transitions between 582 and 602 nm, which is clearly indicative of the presence of two species in solution. Regardless of the emitting wavelength, monoexponential decays were measured with lifetimes in the range 1.06 to 1.16 ms. This behavior was attributed to the presence in solution of a mixture of two distinct coordination environments associated with the square antiprismatic (SAP) and twisted square antiprismatic (TSAP) isomers,[28] which was further confirmed by the observation of characteristic spectral signatures of both species, at 586.5 and 688.0 nm for the SAP isomer, and 689.0 and 681 nm for the TSAP isomer.[27]

The number of coordinated water molecules in [EuL] was determined by using the equation of Beeby and co-workers[17a] and the luminescence decays in H_2O and D_2O [τ_{H2O}=1.11(5) and τ_{D2O}=1.66(2) ms], pointing to a non-hydrated species (q=0.06) in which the Eu^{III} coordination sphere is filled by the four nitrogen atoms of the macrocycle, two nitrogen atoms of the bipyridine unit, and the three oxygen atoms of the acetate arms.

The UV/Vis absorption, excitation, and high-resolution emission spectra of [Eu_2L] in 0.01 MTris-buffered aqueous solutions (pH 7.4) are presented in Figure 6a. The UV/Vis absorption spectrum of [Eu_2L] is very similar to that of [Tb_2L] (Figure 4), with maxima at 301 (ε=10 140 $M^{-1}\,cm^{-1}$) and 236 nm (ε=7 220 $M^{-1}\,cm^{-1}$). Upon excitation into the ππ* absorption bands of the bipyridyl unit, the characteristic emission pattern of Eu^{III} is observed between 575 and 720 nm. The sensitized emission quantum yields were determined in 0.01 M Tris-HCl buffered aqueous solutions at pH 7.4 (ϕ_{H2O}=7.0 %) and in D_2O (ϕ_{D2O}=16 %), using [$Ru(bipy)_3$]Cl_2 in non-degassed water as a reference (ϕ=0.04).[29] Interestingly, a thorough examination of the $^5D_0 \rightarrow {}^7F_0$ transition (Figure 6b) clearly indicates the presence of two components: a maximum at 578.90 nm and a marked shoulder at 578.55 nm. Since this transition is non-degenerate, this pattern is typical of the presence of at least two Eu^{III} sites in solution. The emission spectrum corresponding to the $^5D_0 \rightarrow {}^7F_0$ transitions can be deconvoluted by using two pure Lorentzian functions, which allow the calculation of the emission spectra of each coordination site individually (Figure 6b). The strongest emissive site gives rise to a transition centered at 578.90 nm (63 % of the emitted intensity) and the other site presents a maximum at 578.45 nm (37 %). Considering that the coordination spheres of the two sites differ only by the coordination of the bipyridyl unit for site I or two water molecules for site II (see below), the high-energy component of the $^5D_0 \rightarrow {}^7F_0$ transition can be related to site II, as the nephelauxetic parameters calculated by Horrocks and Frey[30] are more important for N atoms (δ=−12.1 for CN=9) than for coordinated oxygen atoms of water molecules (δ=−10.4 for CN=9). A second remarkable feature of the emission spectrum is the presence of at least five components in the region corresponding to the $^5D_0 \rightarrow {}^7F_1$emission band (583 to 600 nm). This region is composed of a maximum of three sublevels for a single species of low symmetry,[31] and this observation corroborates the presence of two distinct Eu^{III} sites.

A striking result was obtained when water was replaced by D_2O, with the pattern of the emission spectrum of the complex found to be very different (Figure 7). In heavy water, the relative intensities of some of the transitions were greatly increased (see, for example, the transitions at 587.5 and 592.2 nm), while others remained constant (peaks at 585.2 or 680.0 nm).

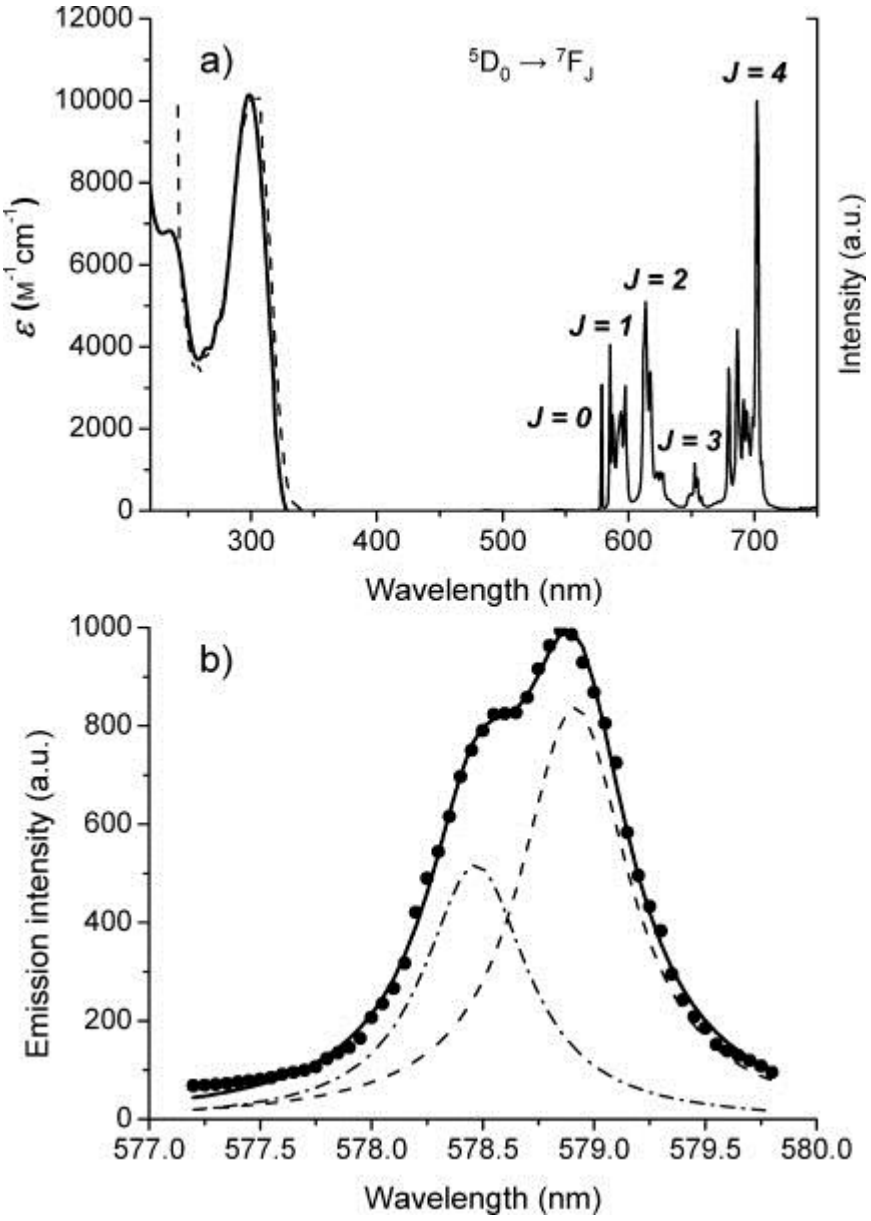

Figure 6. a) UV/Vis absorption (solid line, left part), excitation (dotted lines, λ_{em}=613 nm) and high-resolution emission spectrum (λ_{ex}=300 nm solid line, right part) recorded for [Eu_2L] in 0.01 M Tris-HCl buffered aqueous solutions (pH 7.4, 1.5×10^{-5} M). b) Enlargement of the $^5D_0 \rightarrow {}^7F_0$ region with experimental data [•, fitting to a sum of two Lorentzian peaks (—, R^2=0.998)], and the corresponding individual Lorentzian signals (dashed and dashed–dotted lines).

This behavior can be attributed to the different hydration states for the two distinct Eu^{III}sites (I and II), for which the reduction in vibrational quenching from water to heavy water was translated into a more important luminescence enhancement for the most hydrated Eu site (site II). With the assumption that the thin emission band at 585.2 nm (Figure 7a) can be attributed to one of the Eu sites, and that its relative intensity was unchanged in water and D_2O, this transition was set as a reference transition for site I, and used to determine the shape of the emission pattern of site II, by subtracting the contribution of site I from the spectrum obtained in D_2O (Figure 7b). Considering the non-classical behavior of this complex (see below), it was not possible to estimate the hydration states of each site by classical measurement of the luminescence lifetimes in H_2O and D_2O.[17a] To circumvent this problem, we turned our attention to aqueous mixtures containing the ligand L and Eu^{III} and Gd^{III} cations (as chloride salts) in 1:1.9:0.1 stoichiometry. Assuming that the small ionic contraction has a negligible impact on the conformation of the

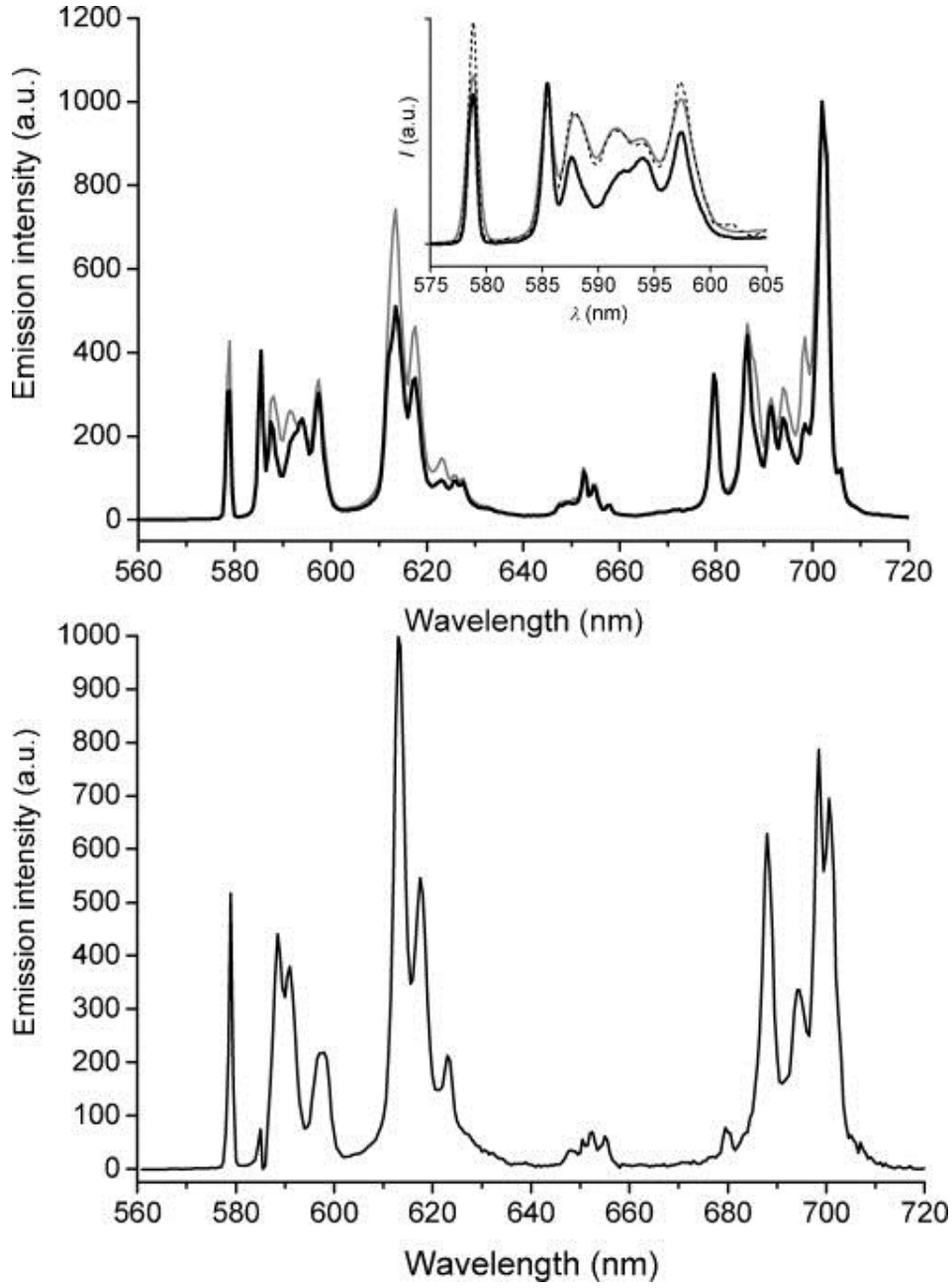

Figure 7. a) Emission spectra (λ_{ex}=300 nm, emission slits=0.5 nm) recorded for [Eu_2L] in 0.01 M Tris-HCl aqueous solution (black, pH 7.4, 1.5×10^{-5} M) and in D_2O solution (gray, 1.5×10^{-5} M), normalized at their maxima. Inset: Zoom on the $^5D_0\rightarrow{}^7F_1$emission band in 0.01 M Tris-HCl aqueous solution (black), in D_2O (gray), and in 0.01 M Tris-HCl upon direct metal excitation at λ_{ex}=396 nm (dotted line). b) Calculated spectrum of the hydrated species.

[Ln_2L] complexes in solution, and that the stability constants for the Eu and Gd complexes are similar, this composition leads to a mixture of [Gd_2L] (90.25 %), [GdEuL] (9.5 % overall, half of it corresponding to Eu in site I) and a minor amount of [Eu_2L] (0.25 %), which could be neglected. The emission spectrum obtained for this mixture of complexes could be superimposed perfectly on that of the [Eu_2L] complex, indicating that the conditions given above are fulfilled. The luminescence decays were then measured in H_2O and D_2O at different wavelengths to obtain information on the hydration number of each site. At 585 nm, a strictly monoexponential decay was obtained with lifetimes of 1.21(3) ms in H_2O and 1.9(1) ms in D_2O, pointing to the absence of inner-sphere water molecules for site I (q=0.1±0.2). These emission lifetimes are very similar to those determined for other coordinatively saturated Eu^{III} complexes,[32] particularly for the case of one based on a do3a moiety functionalized with a 6-methyl-bipyridine moiety

(τ=1.15 ms).[33] At 698 nm, the decay could only be fitted with a biexponential behavior, because the contribution of site I could not be disregarded. By fixing the lifetime corresponding to site I to the value obtained at 585 nm, a lifetime of 0.44(1) ms was obtained for site II. This value lies between those obtained for mono-[34] and bis-hydrated[35] Eu^{III} complexes. Unfortunately, in D_2O, the admixture of emission signals arising from the two sites at 698 nm did not allow unambiguous decomposition into two exponential components, probably as a result of the similar values of the lifetimes for the two sites under these conditions. Assuming that the lifetime in D_2O is close to that obtained for site I, a q value of 1.8±0.2 is obtained, indicating that site II is bis-hydrated. As a convention, sites I and II will be denoted with subscripts 0 and 2 with reference to their hydration states in the following sections.

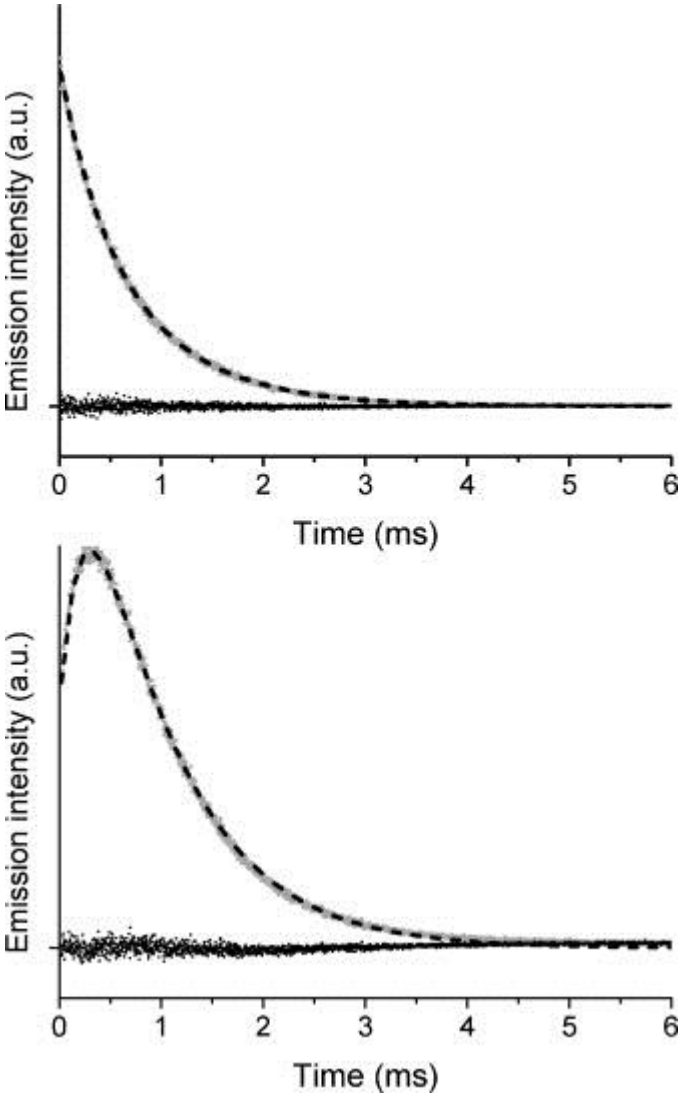

Figure 8. Luminescence intensity profiles (gray) of [Eu_2L] in 0.01 M Tris-HCl at pH 7.4 upon excitation at 300 nm and emission at λ_{em}=585 nm (top) and 698 nm (bottom), and the corresponding fits (dashed lines) and residues (black points).

Intramolecular energy transfer in [Eu_2L]

To gain additional information on the two different coordination sites present in aqueous solution, time-correlated single-photon counting (TCSPC) lifetime measurements were performed at various characteristic emission wavelengths [i.e., 585 nm (Site I), 613 nm (Site I and II), 698 nm (mostly site II), and 702 nm

(mostly site I)] in 0.1 M Tris-HCl at pH 7.4 and in D_2O upon ligand excitation (λ_{exc}=300 nm, Figure 8). Analysis of the data revealed that none of the emission decay profiles were strictly mono- or biexponential, and that two different patterns were obtained depending on the site responsible for the observed transition. The most striking pattern was observed at λ_{em}=698 nm (Figure 8), for which there was a major contribution of the hydrated site (Figure 7). Indeed, this emission decay profile was characterized by an increase in the emission intensity in the first few hundred microseconds, followed by the expected decay of the luminescence. On the contrary, at λ_{em}=585 nm (site I), where the emission intensity is mainly due to the non-hydrated species, a very rapid decay was observed, which was faster than that measured previously for the [$Gd_{1.9}Eu_{0.1}L$] species (see above). All these data strongly suggest energy transfer between the two sites, with the increase in intensity observed at 698 nm (Site II) being assigned to the delayed population of the excited state of the bis-hydrated site, probably due to energy transfer from the non-hydrated site.

The energy transfer between the excited state of the non-hydrated species, Eu_0*, and the excited state of the bis-hydrated species, Eu_2*, can be modeled by the kinetic scheme shown in Scheme 2.

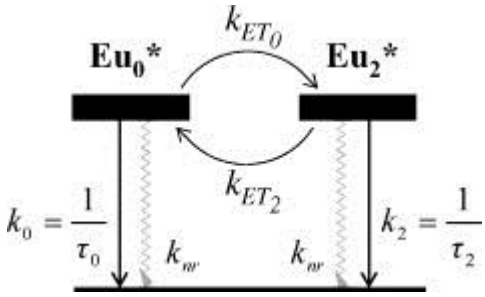

Scheme 2. Kinetic model for the deactivation and energy transfers between the excited levels of **Eu_0*** (q=0) and **Eu_2*** (q=2) in [Eu_2L].

The mathematical treatment of this model leads to the system of differential equations given by Equations (1) and (2), which can be solved to give the time-dependent concentrations of the excited species [Eu_0*] and [Eu_2*] [Eqs. (3) and (4)], in which λ_1, λ_2, v_1, and v_2 can be expressed as polynomial combinations of the luminescence rate constants of the two Eu^{III} centers (k_0 and k_2 for q=0 and q=2, respectively) and of the rate constants of the energy-transfer processes (k_{ET0} and k_{ET2}, respectively) for the transfer from site I to site II and vice versa [Eqs. (5) to (8)]. The full mathematical treatment of this system is presented in the Supporting Information.

$$\frac{d[Eu_2^*(t)]}{dt} = -(k_{ET2} + k_2)[Eu_2^*(t)] + k_{ET0}[Eu_0^*(t)] \quad (1)$$

$$\frac{d[Eu_0^*(t)]}{dt} = -(k_{ET0} + k_0)[Eu_0^*(t)] + k_{ET2}[Eu_2^*(t)] \quad (2)$$

$$[Eu_2^*(t)] = \frac{v_1[Eu_2^*]_0 + v_2[Eu_0^*]_0}{v_1 - v_2} e^{\lambda_1 t} - \frac{v_2}{v_1 - v_2}([Eu_2^*]_0 + [Eu_0^*]_0)e^{\lambda_2 t} \quad (3)$$

$$[Eu_0^*(t)] = ([Eu_2^*]_0 + [Eu_0^*]_0)e^{\lambda_2 t} - [Eu_2^*(t)] \quad (4)$$

$$\lambda_1 = \frac{1}{2}\left(-\sqrt{(k_2 + k_0 + k_{ET0} + k_{ET2})^2 - 4(k_0k_2 + k_2k_{ET0} + k_0k_{ET2})} - (k_0 + k_2 + k_{ET0} + k_{ET2})\right) \quad (5)$$

$$\lambda_2 = \frac{1}{2}\left(\sqrt{(k_2 + k_0 + k_{ET0} + k_{ET2})^2 - 4(k_0k_2 + k_2k_{ET0} + k_0k_{ET2})} - (k_0 + k_2 + k_{ET0} + k_{ET2})\right) \quad (6)$$

$$v_1 = -\frac{1}{k_{ET2}}\left(\frac{1}{2}\left(\sqrt{(k_0 + k_2 + k_{ET0} + k_{ET2})^2 - 4(k_0k_2 + k_0k_{ET2} + k_2k_{ET0})} + k_0 + k_2 + k_{ET0} + k_{ET2}\right) - k_0 - k_{ET0}\right) \quad (7)$$

$$v_2 = -\frac{1}{k_{ET2}}\left(\frac{1}{2}\left(-\sqrt{(k_0 + k_2 + k_{ET0} + k_{ET2})^2 - 4(k_0k_2 + k_0k_{ET2} + k_2k_{ET0})} + k_0 + k_2 + k_{ET0} + k_{ET2}\right) - k_0 - k_{ET0}\right) \quad (8)$$

The measured intensity profiles at 585 and 698 nm were then fitted to Equations (3) and (4) assuming that: 1) the luminescence decays for sites I and II (k_0 and k_2, respectively) are those obtained for the [$Gd_{1.9}Eu_{0.1}L$] complex (1.21 and 0.44 ms, respectively); and 2) the emission at 585 nm arises purely from site I. Through this procedure, the evolution of the emitted intensities at 585 and 698 nm could be fitted well to the sum of two exponential functions, affording values of λ_1 and λ_2 (Figure 8), from which energy-transfer rate constants k_{ET0}=k_{ET2}=0.98 ms^{-1} were obtained.

Ab initio modeling of the [Eu_2L] complex and Förster radii

Attempts to grow single crystals of the [$Ln_2L(H_2O)_2$] complexes presented in this work were unsuccessful. Thus, with the aim of obtaining information concerning the structures of these complexes, we turned our attention to theory. Because of the relatively large sizes of the complexes of interest, our calculations were performed at the HF level. The lanthanides were described by using the quasi-relativistic effective core potential (ECP) of Dolg et al.[36] and the related [5s4p3d]-GTO valence basis set. This ECP includes the 4f electrons in the core, as they are not expected to make a substantial contribution to chemical bonding.

The minimum energy conformation calculated for the [$Ln_2L(H_2O)_2$] (Ln=Eu or Lu) complexes presents a *cis* conformation of the 6,6′-substituted bipyridyl unit (Figure 9),[37] in agreement with the UV spectra described above. According to our calculations, the geometry of the [$Eu_2(L)(H_2O)_2$] complex with SAP coordination around the metal ions is 17.0 kJ mol^{-1} more stable than that corresponding to the TSAP

isomer. The stability of the SAP isomer with respect to the TSAP one increases to 26.5 kJ mol^{-1} for the Lu^{III} complex, in line with the progressive stabilization of the SAP coordination upon moving to the right across the lanthanide series.[38] An SAP coordination environment for these complexes is in perfect agreement with the ^{1}H NMR spectrum of [Yb_2L] described above (Figure 1). One of the Ln^{III}ions is nine-coordinated, being directly bound to the four nitrogen atoms of the cyclen unit, three oxygen atoms of the acetate groups of the do3a cage, and two inner-sphere water molecules. The second metal ion presents a coordination number of eight, which is provided by the four nitrogen atoms of the macrocycle, three oxygen atoms of the acetate groups, and one nitrogen atom of the 6,6′-substituted bipyridyl unit. The distances between the Ln^{III}ion and the second nitrogen atom of the bipy fragment (2.93 and 3.02 Å for the Eu^{III} and Lu^{III}derivatives, respectively) are too long to be considered as bond lengths, but short enough to prevent the possible coordination of a water molecule.

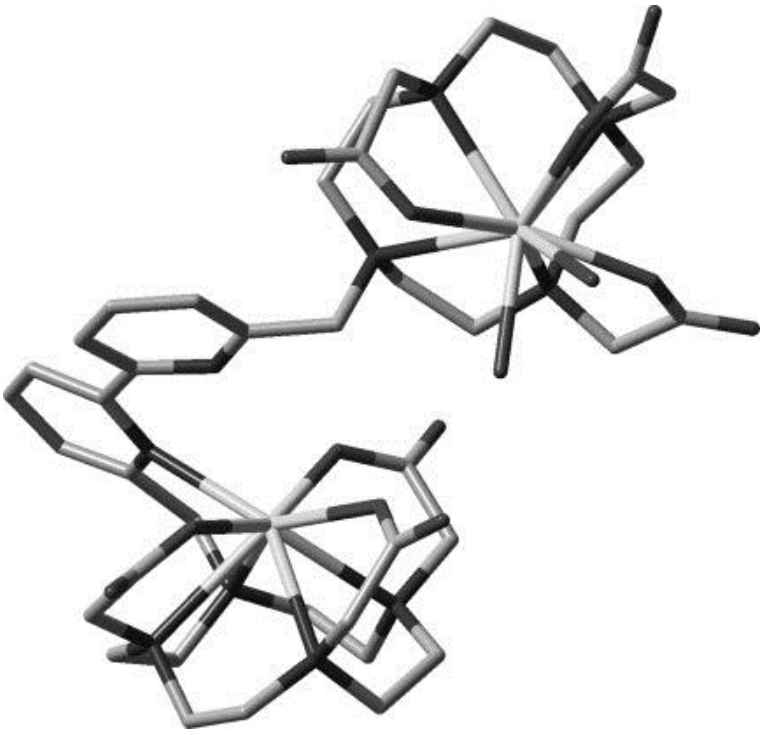

Figure 9. Optimized geometry of the [$Eu_2L(H_2O)_2$] complex obtained from HF calculations. Hydrogen atoms are omitted for the sake of simplicity.

The distances between the Eu^{III} ion and the nitrogen atoms of the macrocycle fall within the range 2.70–2.76 Å for site I, and 2.65–2.83 Å for the Eu^{III} center of site II. The coordinated nitrogen atom of the bipy unit provides a stronger interaction with the Eu^{III} ion than the amine nitrogen atoms (2.60 Å). The distances to the oxygen atoms of carboxylate groups fall within a relatively narrow range (2.29–2.37 Å), whereas the distances between Eu^{III} and the oxygen atoms of inner-sphere water molecules are 2.59 and 2.45 Å. The relatively short value of the latter Eu–O_{water} distance is attributed to the hydrogen-bonding interaction established between one of the hydrogen atoms of the water molecule and a non-coordinated oxygen atom of one of the acetate groups of the neighboring do3a cage. The calculated Eu–O bond lengths are very close to those observed in the solid state for complexes with do3a and dota derivatives, whereas the calculated Eu–N distances are typically 0.05–0.10 Å longer than those observed in the solid state.[39] For the [Lu_2L] complex, our calculations provide very similar coordination environments around the metal ions, although the bond lengths of the metal coordination sphere are obviously shorter than for the [Eu_2L] complex as a

consequence of the lanthanide contraction.[40] The calculated intramolecular $Ln^{III}\cdots Ln^{III}$ distances are 7.05 and 7.16 Å for the Eu and Lu complexes, respectively.

The calculated intramolecular $Eu^{III}\cdots Eu^{III}$ distance, *r*, was used to calculate the Förster radii, R_0, the distance at which 50 % of the energy of the donor is transferred to the acceptor for the two donor/acceptor pairs (depending whether Eu_0 or Eu_2 is considered as the donor), according to Equation (9), in which τ_D is the lifetime of the donor in the absence of the acceptor.[41,13e]

$$k_{ET} = \frac{1}{\tau_D}\left(\frac{R_0}{r}\right)^6 \qquad (9)$$

Values of $R_{0(0\rightarrow 2)}$=8.1 Å and $R_{0(2\rightarrow 0)}$=6.8 Å were calculated, highlighting the larger efficiency of the energy transfer from site I to site II compared to the reverse situation, and explaining why it was possible to observe a rise in intensity at certain wavelengths for which the contribution of site II was predominant. It should also be noted that these values are in good agreement with values reported in the literature for energy transfer between different lanthanide cations obtained by direct calculation of the integral overlap from spectroscopic data (≈6 Å for Eu-to-Nd energy transfer in bis-dota-type complexes,[42] 8.5 and 8.9 Å, respectively, for Eu-to-Pr and Eu-to-Nd in protein systems),[43] or by lifetime analysis (10.7 Å for Tb-to-Eu transfer in heterodinuclear triple helices).[44]

Conclusion

The successive complexation of two lanthanide cations to ligand L resulted in the formation of a dissymmetric dinuclear [Ln_2L] complex, in which the two metal ions possess different coordination environments. Both metal ions are bound directly to seven heteroatoms per do3a unit, their coordination spheres being completed by a nitrogen atom of the bipyridyl unit for the first site or by two water molecules for the second site. The close proximity of the two lanthanide cations allowed the observation of an unprecedented Eu-to-Eu energy-transfer phenomenon within a discrete complex in solution. The energy transfer is translated into unconventional behavior of the time-dependent luminescence intensity, which, for the hydrated site, shows a rising step of the luminescence intensity during the very first hundreds of microseconds after the pulsed excitation. It should be emphasized that, although such a process is probably also present in the case of the [Tb_2L] complex, the weaker influence of the coordinated water molecules on the emission intensity[17] and the complicated emission pattern characteristics of Tb^{III} did not allow the unequivocal establishment of the occurrence of intramolecular ET. However, in the case of the [Eu_2L] complex, our results confirm that a Eu^{III}-centered excited state can be populated either by direct photosensitization through the antenna unit or by energy transfer from a proximal Eu^{III} site, which opens very interesting opportunities such as the possibility to bring excess energy to an excited state, potentially resulting in energy up-conversion processes within discrete molecular entities in solution.[15a]

Experimental section

General methods

Elemental analyses were carried out on a Carlo Erba 1108 elemental analyzer. High-resolution ESI-TOF mass spectra were recorded using an LC-Q- TOF Applied Biosystems QSTAR Elite spectrometer in the

positive mode. IR spectra were recorded using a Bruker Vector 22 spectrophotometer equipped with a Golden Gate Attenuated Total Reflectance (ATR) accessory (Specac). ^{1}H and ^{13}C NMR spectra were recorded at 25 °C on Bruker Avance 300 and Bruker Avance 500 MHz spectrometers. For measurements in D_2O, *tert*-butyl alcohol was used as an internal standard with the methyl signal calibrated at δ=1.2 (^{1}H) and 31.2 ppm (^{13}C).

UV/Vis absorption spectra were recorded on a Specord 205 (Analytik Jena) spectrometer. Steady-state emission and excitation spectra were recorded on a Horiba Jobin Yvon Fluorolog 3 spectrometer working with a continuous 450 W Xe lamp. For the measurements in the solid state, the spectrometer was fitted with an integrating sphere Quanta-Φ from Horiba. Detection was performed with a Hamamatsu R928 photomultiplier. All spectra were corrected for the instrumental functions. When necessary, a 399 nm cutoff filter was used to eliminate second-order artifacts. Phosphorescence lifetimes were measured on the same instrument working in phosphorescence mode, with a 50 μs delay time and a 100 ms integration window, or in the TCSPC lifetime spectroscopy mode, both using a Xenon flash lamp as the excitation source.

Monoexponential and biexponential emission decay profiles were fitted with the FAST program from Edinburgh Instruments or with the Datastation software from Jobin Yvon. Hydration numbers, *q*, were obtained using Equation (10),[17a] in which τ_{H2O} and τ_{D2O} refer to the measured luminescence decay lifetimes (in ms) in water and deuterated water, respectively, using A_{Eu}=1.2 and a_{Eu}=0.25 for Eu^{III}, and A_{Tb}=5.0 and a_{Tb}=0.06 for Tb^{III}.

$$q = A_{Ln}\left(1/\tau_{H_2O} - 1/\tau_{D_2O} - a_{Ln}\right) \quad (10)$$

Luminescence quantum yields were measured according to conventional procedures, with diluted solutions (optical density < 0.05), using $[Ru(bipy)_3]Cl_2$ in non-degassed water (Φ=4.0 %),[29] and rhodamine 6G in water (Φ=76.0 %)[26] as references. The estimated errors were ±15 %.

Solid-state studies and quantum yields were determined using an absolute method with the integrating sphere. The quantum yield in the absolute method can be calculated using Equation (11).

$$\phi = \frac{N_{emission}}{N_{absorption}} = \frac{\int \frac{\lambda}{hc}\left\{I_{em}^{sam}(\lambda) - I_{em}^{ref}(\lambda)\right\}d\lambda}{\int \frac{\lambda}{hc}\left\{I_{ex}^{ref}(\lambda) - I_{ex}^{sam}(\lambda)\right\}d\lambda} \quad (11)$$

Here, $N_{absorption}$ is the number of photons absorbed by the sample and $N_{emission}$ is the number of photons emitted from the sample, λ is the wavelength, *h* is Planck's constant, *c* is the velocity of light, I_{ex}^{sam} and I_{ex}^{ref} are the integrated intensities of the excitation light with and without the sample, respectively, and I_{em}^{sam} and I_{em}^{ref} are the photoluminescence intensities with and without the sample, respectively. This method has been described in detail by L. S. Rohwer and J. E. Martin.[45]

Chemicals and starting materials

6,6′-Bis(bromomethyl)-2,2′-bipyridine (**1**) was prepared according to the literature method.[46] All other chemicals were purchased from commercial sources and used without further purification, unless otherwise stated. Neutral Al_2O_3 (Fluka, 0.05–0.15 mm) was used for preparative column chromatography.

6,6′-Bis(4,7,10-tris(tert-butoxycarbonylmethyl)-1,4,7,10-tetraazacyclododecane-1-ylmethyl)-2,2′-bipyridine (2)

A mixture of do3a(tBuO)$_3$ (0.500 g, 0.971 mmol) and Na_2CO_3(0.211 g, 1.99 mmol) in acetonitrile (25 mL) was stirred for 30 min, and then 6,6′-bis(bromomethyl)-2,2′-bipyridine (0.166 g, 0.486 mmol) and a catalytic amount of KI were added. The mixture was heated to reflux with stirring under an inert atmosphere (Ar) for a period of 24 h, and then the excess Na_2CO_3 was filtered off. The filtrate was concentrated to dryness and the yellow oil was extracted with a 1:3 mixture of H_2O and CH_2Cl_2 (100 mL). The organic phase was evaporated to dryness to give an oily residue that was purified by column chromatography on Al_2O_3 with a CH_2Cl_2/MeOH 5 % mixture as the eluent to give **1** (0.535 g) as a yellow foam. Yield: 85 %. Elemental analysis calcd (%) for $C_{64}H_{108}N_{10}O_{12}\cdot CH_2Cl_2$: C 60.31, H 8.56, N 10.82; found: C 60.32, H 8.42, N 10.67; MS (ESI$^+$): *m/z* 1210 ($[C_{64}H_{109}N_{10}O_{12}]^+$) and 605 ($[C_{64}H_{110}N_{10}O_{12}]^{2+}$); IR (ATR): $\tilde{\nu}$=1721 (C=O), 1579 cm^{-1} (C=N); ^{1}H NMR ($CDCl_3$, 500 MHz, 25 °C, TMS): δ=8.74 (s, 2 H), 7.73 (t, 2 H, ^3J=7.6 Hz), 7.38 (d, 2 H, ^3J=7.5 Hz), 3.75–1.89 (m, 48 H, -NCH_2), 1.46–1.42 ppm (m, 54 H, tBuO-); ^{13}C NMR ($CDCl_3$, 125.8 MHz, 25 °C, TMS): δ=172.9, 172.4, 156.7, 156.1, 137.4, 125.8, 120.1, 82.1, 81.2, 60.1, 56.6, 56.4, 56.0, 53.4, 51.7, 49.8, 48.8, 48.5, 31.8, 28.1, 28.0, 27.8 ppm.

6,6′-Bis(4,7,10-tris(carboxymethyl)-1,4,7,10-tetraazacyclododecane-1-ylmethyl)-2,2′-bipyridine hexatrifluoroacetate (H_6L)

Compound **2** (0.535 g, 0.413 mmol) was dissolved in a 1:1 mixture of water and trifluoroacetic acid (10 mL). The mixture was heated to reflux with stirring for 24 h, and then the solvents were removed in a rotary evaporator to give a brown oil. This was dissolved in MeOH (10 mL) and the solvent was evaporated. This process was repeated twice, and then three times with CH_2Cl_2. The oily residue was dissolved in MeOH (1 mL), and diethyl ether was added until the precipitation of a white solid was complete. The white solid was isolated by filtration and dried under vacuum to give 0.498 g of the desired compound. Yield: 75 %. Elemental analysis calcd (%) for $C_{40}H_{60}N_{10}O_{12}\cdot 6\,CF_3COOH\cdot 3\,H_2O$: C 38.76, H 4.50, N 8.69; found: C 39.04, H 4.37, N 8.86; MS (ESI$^+$): *m/z* 873 ($[C_{40}H_{61}N_{10}O_{12}]^+$) and 437 ($[C_{40}H_{62}N_{10}O_{12}]^{2+}$); IR (ATR): $\tilde{\nu}$=3436 (O-H), 1673 and 1678 (C=O), 1584 cm^{-1} (C=N); ^{1}H NMR (D_2O, pD 2.1, 500 MHz, 25 °C, TMS): δ=8.68–7.78 (m, 6 H), 4.40–2.86 ppm (m, 48 H); ^{13}C NMR (D_2O, pD 2.1, 125.8 MHz, 25 °C, TMS): δ=176.6, 176.0, 170.8, 156.4, 149.7, 142.7, 129.8, 125.6, 59.8, 57.2, 56.1, 55.3, 54.6, 53.6, 53.3, 52.6, 50.8, 50.5, 50.1, 49.2 ppm.

General procedure for the preparation of $[Ln_2L]\cdot 4\,H_2O$ complexes

A mixture of $L\cdot 6\,CF_3COOH\cdot 3\,H_2O$ (0.100 g, 0.062 mmol), triethylamine (0.075 g, 0.744 mmol), and Ln(OTf)$_3$(0.124 mmol, Ln=Eu, Gd, Tb, Yb, or Lu) in 2-propanol (10 mL) was heated to reflux for 24 h. The reaction was allowed to cool to room temperature, resulting in the formation of a white precipitate that was washed with MeOH and diethyl ether. The mother liquor was stored at 4 °C for several days, resulting in the formation of a second batch of complex, which was again collected by filtration and washed with MeOH and diethyl ether.

$[Eu_2L]\cdot 4\,H_2O$: Yield: 0.062 g, 81 %; elemental analysis calcd (%) for $C_{40}H_{54}Eu_2N_{10}O_{12}\cdot 4\,H_2O$: C 38.65, H 5.03, N 11.27; found: C 38.78, H 5.26, N 10.98; HS-MS (ESI$^+$): *m/z* 587.1257; calcd for $[C_{40}H_{56}Eu_2N_{10}O_{12}]^{2+}$ 587.1246; *m/z* 1173.2373; calcd for $[C_{40}H_{55}Eu_2N_{10}O_{12}]^+$ 1173.2420; IR (ATR): $\tilde{\nu}$=1579 cm^{-1} (C=O).

$[Gd_2L]\cdot 4\,H_2O$: Yield: 0.065 g, 83 %; elemental analysis calcd (%) for $C_{40}H_{54}Gd_2N_{10}O_{12}\cdot 4\,H_2O$: C 38.33, H 4.99, N 11.17; found: C 38.18, H 4.81, N 10.98; HS-MS (ESI^+): *m/z* 592.1284; calcd for $[C_{40}H_{56}Gd_2N_{10}O_{12}]^{2+}$ 592.1275; *m/z* 1183.2457; calcd for $[C_{40}H_{55}Gd_2N_{10}O_{12}]^+$ 1183.2477; IR (ATR): $\tilde{\nu}$=1582 cm^{-1} (C=O).

$[Tb_2L]\cdot 4\,H_2O$: Yield: 0.062 g, 79 %; elemental analysis calcd (%) for $C_{40}H_{54}N_{10}O_{12}Tb_2\cdot 4\,H_2O$: C 38.23, H 4.97, N 11.14; found: C 38.39, H 4.90, N 11.33; HS-MS (ESI^+): *m/z* 593.1279; calcd for $[C_{40}H_{56}N_{10}O_{12}Tb_2]^{2+}$ 593.1287; *m/z* 1185.2535; calcd for $[C_{40}H_{55}N_{10}O_{12}Tb]^+$ 1185.2502; IR (ATR): $\tilde{\nu}$=1580 cm^{-1} (C=O).

$[Yb_2L]\cdot 4\,H_2O$: Yield: 0.068 g, 85 %; elemental analysis calcd for $C_{40}H_{54}N_{10}O_{12}Yb_2\cdot 4\,H_2O$: C 37.39, H 4.86, N 10.90; found: C 37.48, H 5.03, N 11.05; HS-MS (ESI^+): *m/z* 608.1441; calcd for $[C_{40}H_{56}N_{10}O_{12}Yb_2]^{2+}$ 608.1422; *m/z* 1215.2717; calcd for $[C_{40}H_{55}N_{10}O_{12}Yb_2]^+$ 1215.2772; IR (ATR): $\tilde{\nu}$=1589 cm^{-1} (C=O).

$[Lu_2L]\cdot 4\,H_2O$: Yield: 0.062 g, 77 %; elemental analysis calcd (%) for $C_{40}H_{54}Lu_2N_{10}O_{12}\cdot 4\,H_2O$: C 37.27, H 4.85, N 10.87; found: C 37.44, H 4.73, N 10.65; HS-MS (ESI^+): *m/z* 609.1457; calcd for $[C_{40}H_{56}Lu_2N_{10}O_{12}]^{2+}$ 609.1441; *m/z* 1217.2792; calcd for $[C_{40}H_{55}Lu_2N_{10}O_{12}]^+$ 1217.2811; IR (ATR): $\tilde{\nu}$=1589 cm^{-1} (C=O); ^{13}C NMR (D_2O, pD 7.0, 125.8 MHz, 25 °C, TMS): δ=183.3, 182.8, 182.7, 182.0, 181.5, 180.5, 161.3, 159.5, 157.3, 156.3, 143.8, 140.5, 130.2, 126.6, 124.9, 124.5, 68.2, 68.1, 68.0, 67.8, 67.6, 67.5, 67.1, 66.4, 59.4, 58.6, 58.1, 57.8, 57.7, 57.5, 57.3, 57.2, 56.9, 56.7, 56.6, 56.5, 55.0, 53.8, 47.4, 46.8 ppm.

Computational methods

All calculations were performed employing the Gaussian 09 package (Revision C.01).[47] Full geometry optimizations of the $[Ln_2L(H_2O)_q]$ systems (q=1, 2; Ln=Eu, Gd, or Lu) were performed at the HF level by using the effective core potential (ECP) of Dolg et al. and the related [5s4p3d]-GTO valence basis set for the lanthanides,[36] and the 3–21G basis set for C, H, N, and O atoms. Although small, HF calculations employing this basis set in combination with the f-in-core ECP of Dolg were shown to provide molecular geometries of Ln^{III} dota-like complexes, in good agreement with the experimental structures observed by single-crystal X-ray diffraction studies.[49] No symmetry constraints were imposed during the optimizations. The stationary points found on the potential energy surfaces as a result of the geometry optimizations were tested to represent energy minima rather than saddle points using frequency analysis. The relative free energies of the different conformations obtained from geometry optimizations were calculated at the same computational level, and they include non-potential-energy contributions (zero-point energies and thermal terms) obtained through frequency analysis. Selected geometries optimized at the HF level were subsequently fully optimized by using hybrid DFT with the B3LYP exchange-correlation functional,[48,50] and the standard 6–31G(d) basis set for the ligand atoms. Because of the considerable computational effort involved in the calculation of second derivatives at this level, the optimized geometries were not characterized by using frequency analysis. A comparison of the molecular geometries optimized at the HF and B3LYP levels shows that both models provide very similar coordination environments around the Ln^{III} ion.

Acknowledgements

We gratefully acknowledge Prof. David Parker for fruitful discussions and comments on this work. M. R.-F., D. E.-G., A. de B., T. R.-B., and C. P.-I. thank Ministerio de Educación y Ciencia (MEC, CTQ2009–10721), Fondo Europeo de Desarrollo Regional (FEDER, CTQ2009–10721) and Xunta de

Galicia(IN845B-2010/063) for financial support. This research was performed in the framework of the EU COST ActionD38 “Metal-Based Systems for Molecular Imaging Applications”. The authors are indebted to Centro de Supercomputación de Galicia (CESGA) for providing the computer facilities. A. N. and L. J. C. gratefully acknowledge the financial support of the French Centre National de la Recherche Scientifique and the University of Strasbourg.

References

[1] J. Deisenhofer, O. Epp, K. Miki, R. Huber, H. Michel, *J. Mol. Biol.* **1984**, *180*, 385–398.

[2] J. D. Scholes, G. R. Fleming, A. Olaya-Castro, R. van Grodelle, *Nat. Chem.* **2011**, *3*, 763–774.

[3] a) T. M. Swager, *Acc. Chem. Res.* **1998**, *31*, 201; b) J. H. Wosnick, T. M. Swager, *Curr. Opin. Chem. Biol.* **2000**, *4*, 715–720.

[4] Q. Zhou, T. H. Swager, *J. Am. Chem. Soc.* **1995**, *117*, 12593–12602.

[5] M. J. Currie, J. K. Mapel, T. D. Heidel, S. Goffri, M. A. Baldo, *Science* **2008**, *321*, 226–228.

[6] a) H. Barnhill, S. Claudel-Gillet, R. Ziessel, L. J. Charbonnière, Q. Wang, *J. Am. Chem. Soc.* **2007**, *129*, 7799–7806; b) L. J. Charbonnière, N. Hildebrandt, R. Ziessel, H.-G. Löhmannsröben, *J. Am. Chem. Soc.* **2006**, *128*, 12800–12809.

[7] a) T. L. Jennings, S. G. Becker-Catania, R. C. Triulzi, G. Tao, B. Scott, K. E. Sapsford, S. Spindel, E. Oh, V. Jain, J. B. Delehanty, D. E. Prasuhn, K. Boeneman, R. Algar, I. L. Medintz, *ACS Nano* **2011**, *5*, 5579–5593; b) E. R. Goldman, A. R. Clapp, G. P. Anderson, H. T. Uyeda, J. M. Mauro, I. L. Medintz, H. Mattoussi, *Anal. Chem.* **2004**, *76*, 684–688; c) D. Geißler, L. J. Charbonnière, R. Ziessel, N. G. Butlin, H.-G. Löhmannsröben, N. Hildebrandt, *Angew. Chem.* 2010, **122**, 1438–1443; *Angew. Chem. Int. Ed.* **2010**, *49*, 1396–1401.

[8]T. Miyakawa, D. L. Dexter, *Phys. Rev.* **1970**, *B1*, 2961.

[9] T. Förster, *Disc. Faraday Soc.* **1959**, *27*, 7.

[10] D. L. Dexter, *J. Chem. Phys.* **1953**, *21*, 836.-850.

[11] see for example a) G. L. Closs, M. D. Johnson, J. R. Miller, P. Piotrowiak, *J. Am. Chem. Soc.* **1989**, *111*, 3751–3753; b) H. Oevering, J. W. Verhoeven, M. N. Paddon-Row, E. Cotsaris, N. S. Hush, *Chem. Phys. Lett.***1988**, *143*, 488–495; c) D. Gust, T. A. Moore, *Science* **1989**, *244*, 35–41; d) N. Kimizuka, T. Kunitake, *J. Am. Chem. Soc.* **1989**, *111*, 3758–3759.

[12] For example, see: a) H. Imahori, K. Hagiwara, M. Aoki, T. Akiyama, S. Taniguchi, T. Okada, M. Shirakawa, Y. Sakata, *J. Am. Chem. Soc.* **1996**, *118*, 11771–11782; b) B. Alpha, J.-M. Lehn, G. Mathis, *Angew. Chem.* **1987**, *99*, 259–261; *Angew. Chem. Int. Ed. Engl.* **1987**, *26*, 266–267; c) M. Starck, P. Kadjane, E. Bois, B. Darbouret, A. Incamps, R. Ziessel, L. J. Charbonnière, *Chem. Eur. J.* **2011**, *17*, 9164–9179.

[13] a) F. Barigelletti, L. Flamigni, M. Guardigli, A. Juris, M. Beley, S. Chodorowski-Kimmes, J.-P. Collin, J.-P. Sauvage, *Inorg. Chem.* **1996**, *35*, 136–142; b) V. Balzani, A. Credi, F. Scandola, in *Transition Metals in Supramolecular Chemistry*, (Eds.: L. Fabbrizi, A. Poggi), Kluwer Academic Publishers, Dordrecht, **1994**, pp. 1–32; c) F. Scandola, V. Balzani, *J. Chem. Educ.* **1983**, *60*, 814–823; d) P.

Froidevaux, J.-C. G. Bünzli, *J. Phys. Chem.* **1994**, *98*, 532–536; e) L. J. Charbonnière, N. Hildebrandt, *Eur. J. Inorg. Chem.* **2008**, 3241–3251.

[14] T. N. Singh-Rachford, F. N. Castellano, *Coord. Chem. Rev.* **2010**, *254*, 2560–2573.

[15] a) L. Aboshyan-Sorgho, C. Besnard, P. Pattison, K. R. Kittilstved, A. Aebischer, J.-C. G. Bünzli, A. Hauser, C. Piguet, *Angew. Chem.* **2011**, *123*, 4194–4198; *Angew. Chem. Int. Ed.* **2011**, *50*, 4108–4112; b) S. Sivakumar, F. C. J. M. van Veggel, P. S. May, *J. Am. Chem. Soc.* **2007**, *129*, 620–625.

[16] a) J.-C. G. Bünzli, C. Piguet, *Chem. Soc. Rev.* **2005**, *34*, 1048–1077; b) A. de Bettencourt-Dias, *Curr. Org. Chem.* **2007**, *11*, 1460–1480.

[17] a) A. Beeby, I. M. Clarkson, R. S. Dickins, S. Faulkner, D. Parker, L. Royle, A. S. de Sousa, J. A. G. Williams, M. Woods, *J. Chem. Soc. Perkin Trans. 2* **1999**, 493–503; b) R. M. Supkowski, W. D. Horrocks, Jr., *Inorg. Chim. Acta* **2002**, *340*, 44–48; c) Y. Hasegawa, Y. Kimura, K. Murakoshi, Y. Wada, J.-H. Kim, N. Nakashima, T. Yamanaka, S. Yanagida, *J. Phys. Chem.* **1996**, *100*, 10201–10205; d) Y. Hasegawa, K. Murakoshi, Y. Wada, S. Yanagida, J.-H. Kim, N. Nakashima, T. Yamanaka, *Chem. Phys. Lett.* **1996**, *248*, 8–12.

[18] M. Laberge, D. J. Simkin, G. Boulon, A. Monteil, *J. Lumin.* **1993**, *55*, 159–166.

[19] A. L. Barge, Tei, D. Upadhyaya, F. Fedeli, L. Beltrami, R. Stefania, S. Aime, G. Cravotto, *Org. Biomol. Chem.* **2008**, *6*, 1176–1184.

[20] M. Regueiro-Figueroa, D. Esteban-Gómez, A. de Blas, T. Rodríguez-Blas, C. Platas-Iglesias, *Eur. J. Inorg. Chem.* **2010**, 3586–3595.

[21] a) L. S. Natrajan, A. J. L. Villaraza, A. M. Kenwright, S. Faulkner, *Chem. Commun.* **2009**, 6020–6022; b) M. Main, M. M. Meloni, M. Jauregui, D. Sykes, S. Faulkner, A. M. Kenwright, J. S. Snaith, *Chem. Commun.* **2008**, 5212–5214.

[22] a) K. Nakamoto, *J. Phys. Chem.* **1960**, *64*, 1420; b) P. Krumholz, *J. Am. Chem. Soc.* **1951**, *73*, 3487; c) V. Kubíček, A. Hamplová, L. Maribé, S. Mameri, R. Ziessel, É. Tóth, L. Charbonnière, *Dalton Trans.* **2009**, 9466–9474.

[23] H. Gampp, M. Maeder, C. J. Meyer, A. D. Zuberbühler, *Talanta* **1985**, *32*, 251264.

[24] W. P. Cacheris, S. K. Nickle, A. D. Sherry, *Inorg. Chem.* **1987**, *26*, 958–960.

[25] J.-C. G. Bünzli, *Chem. Rev.* **2010**, *110*, 2729–2755.

[26] J. Olmsted III, *J. Phys. Chem.* **1979**, *83*, 2581–2584.

[27] D. Sadhukhan, A. Ray, G. Pilet, G. M. Rosair, E. Garriba, A. Nonat, L. J. Charbonnière, S. Mitra, *Bull. Chem. Soc. Jpn.* **2011**, *84*, 764–777.

[28] a) A. Borel, J. F. Bean, R. B. Clarkson, L. Helm, L. Moriggi, A. D. Sherry, M. Woods, *Chem. Eur. J.* **2008**, *14*, 2658–2667; b) G. Muller, S. D. Kean, D. Parker, J. P. Riehl, *J. Phys. Chem. A* **2002**, *106*, 12349–12355; c) L. M. P. Lima, A. Lecointre, J.-F. Morfin, A. de Blas, D. Visvikis, L. J. Charbonnière, C. Platas-Iglesias, R. Tripier, *Inorg. Chem.* **2011**, *50*, 12508–12521.

[29] H. Ishida, S. Tobita, Y. Hasegawa, R. Katoh, K. Nozaki, *Coord. Chem. Rev.* **2010**, *254*, 2449–2458.

[30] S. T. Frey, W. D. Horrocks, *Inorg. Chim. Acta* **1995**, *229*, 383–390.

[31] S. V. Eliseeva, J.-C. G. Bünzli, *Chem. Soc. Rev.* **2010**, *39*, 189–227.

[32] a) B. Song, G. Wang, J. Yuan, *Chem. Commun.* **2005**, 3553–3555; b) J.-M. Senegas, G. Bernardinelli, D. Imbert, J.-C. G. Bünzli, P.-Y. Morgantini, J. Weber, C. Piguet, *Inorg. Chem.* **2003**, *42*, 4680–4695; c) M. Giraud, E. S. Andreiadis, A. S. Fisyuk, R. Demadrille, J. Pécaut, D. Imbert, M. Mazzanti, *Inorg. Chem.* **2008**, *47*, 3952–3955; d) P. Kadjane, M. Starck, F. Camerel, D. Hill, N. Hildebrandt, R. Ziessel, L. J. Charbonnière, *Inorg. Chem.* **2009**, *48*, 4601–4603; e) S. Quici, G. Marzanni, M. Cavazzini, P. L. Anell, M. Botta, E. Gianolo, G. Accorsi, N. Armaroli, F. Barigeletti, *Inorg. Chem.* **2002**, *41*, 2777–2784.

[33] J. P. Cross, A. Dadabhoy, P. J. Sammes, *J. Lumin.* **2004**, *110*, 113–124.

[34] a) P. Atkinson, Y. Bretonnière, D. Parker, *Chem. Commun.* **2004**, 438–439; b) I. Nasso, C. Galaup, F. Havas, P. Tisnès, C. Picard, S. Laurent, Vander L. Elst, R. N. Muller, *Inorg. Chem.* **2005**, *44*, 8293–8305; c) A. Beeby, L. M. Bushby, D. Maffeo, J. A. G. Williams, *Dalton Trans.* **2002**, 48–54; d) N. Weibel, L. J. Charbonnière, M. Guardigli, A. Roda, R. Ziessel, *J. Am. Chem. Soc.* **2004**, *126*, 4888–4896; e) P. Atkinson, K. S. Findlay, F. Kielar, R. Pal, D. Parker, R. A. Poole, H. Puschmann, S. L. Richardson, P. A. Stenson, A. L. Thompson, J. Yu, *Org. Biomol. Chem.* **2006**, *4*, 1707–1722.

[35] a) A. Dadabhoy, S. Faulkner, P. G. Sammes, *Perkin Trans. 2* **2000**, 2359–2360; b) L. J. Charbonnière, N. Weibel, P. R. Retailleau, R. Ziessel, *Chem. Eur. J.* **2007**, *13*, 346–358; c) J.-M. Siaugue, F. Segat-Dioury, A. Favre-Réguillon, C. Madic, J. Foos, A. Guy, *Tetrahedron Lett.* **2000**, *41*, 7443–7446; d) L. J. Charbonnière, S. Mameri, P. Kadjane, C. Platas-Iglesias, R. Ziessel, *Inorg. Chem.* **2008**, *47*, 3748–3762.

[36] M. Dolg, H. Stoll, A. Savin, H. Preuss, *Theor. Chim. Acta* **1989**, *75*, 173–194.

[37] The relative free energies of the *trans* isomers with respect to the *cis* ones amount to 40.7 (Eu^{III}, SAP), 47.4 (Eu^{III}, TSAP), 39.9 (Lu^{III}, SAP) and 39.9 kJ mol^{-1} (Lu^{III}, TSAP).

[38] a) S. Aime, M. Botta, M. Fasano, M. P. M. Marques, C. F. G. C. Geraldes, D. Pubanz, A. E. Merbach, *Inorg. Chem.* **1997**, *36*, 2059–2068; b) M. Purgel, Z. Baranyai, A. de Blas, T. Rodríguez-Blas, I. Bányai, C. Platas-Iglesias, I. Tóth, *Inorg. Chem.* **2010**, *49*, 4370–4382.

[39] a) S. Aime, A. S. Batsanov, M. Botta, J. A. K. Howard, M. P. Lowe, D. Parker, *New J. Chem.* **1999**, *23*, 669–670; b) C. A. Chang, L. C. Francesconi, M. F. Malley, K. Kumar, J. Z. Gougoutas, M. F. Tweedle, Wilson, L. J. D. W. Lee, *Inorg. Chem.* **1993**, *32*, 3501–3508; c) S. Aime, P. L. Anelli, M. Botta, F. Fedeli, M. Grandi, Uggeri. F. P. Paoli, *Inorg. Chem.* **1992**, *31*, 2422–2428; d) J. Platzek, P. Blaszkiewicz, H. Gries, P. Luger, G. Michl, A. Muller-Fahrnow, B. Raduchel, D. Sulzle, *Inorg. Chem.* **1997**, *36*, 6086–6093; e) K. Kumar, C. A. Chang, L. C. Francesconi, D. D. Dischino, M. F. Malley, Tweedle. M. F. J. Z. Gougoutas, *Inorg. Chem.* **1994**, *33*, 3567–3575.

[40] M. Seitz, A. G. Oliver, K. N. Raymond, *J. Am. Chem. Soc.* **2007**, *129*, 11153–11160.

[41] B. Valeur, in *Molecular Fluorescence: Principles and Applications*, Wiley-VCH, Weinheim, **2002**.

[42] C. M. Andolina, J. R. Morrow, *Eur. J. Inorg. Chem.* **2011**, *1*, 154–164.

[43] W. D. W. Horrocks, M.-J. Rhee, A. P. Snyder, D. R. Sudnick, *J. Am. Chem. Soc.* **1980**, *102*, 3650–3652.

[44] C. Piguet, J.-C. G. Bünzli, G. Bernardnelli, G. Hopfgartner, A. F. Williams, *J. Am. Chem. Soc.* **1993**, *115*, 8197–8206.

[45] L. S. Rohwer, J. E. Martin, *J. Lumin.* **2005**, *115*, 77–90.

[46] P. U. Maheswari, K. Lappalainen, M. Sfregola, S. Barends, P. Gamez, U. Turpeinen, I. Mutikainen, G. P. van Wezel, J. Reedijk, *Dalton Trans.* **2007**, 3676- 3683.

[47] M. J. Frisch, et al. Gaussian 09, Revision A.01, Gaussian, Inc., Wallingford CT, **2009**.

[48] A. D. Becke, *J. Chem. Phys.* **1993**, *98*, 5648–5652.

[49] U. Cosentino, A. Villa, D. Pitea, G. Moro, V. Barone, A. Maiocchi, *J. Am. Chem. Soc.* **2002**, *124*, 4901–4909.

[50] C. Lee, W. Yang, R. G. Parr, *Phys. Rev. B* **1988**, *37*, 785–789.

[i] Supporting information for this article is available online: https://doi.org/10.1002/chem.201200087.